BENDING OF CARBON NANOTUBES ROPES

Veturia Chiroiu (veturiachiroiu@yahoo.com)
Institute of Solid Mechanics of Romanian Academy

Petre P. Teodorescu
(petre_teodorescu@hotmail.com)
University of Bucharest

Ligia Munteanu (ligia_munteanu@ hotmail.com
Institute of Solid Mechanics of Romanian Academy

Viorel-Puiu Paun (paun@physics.pub.ro)
University Politehnica from Bucharest

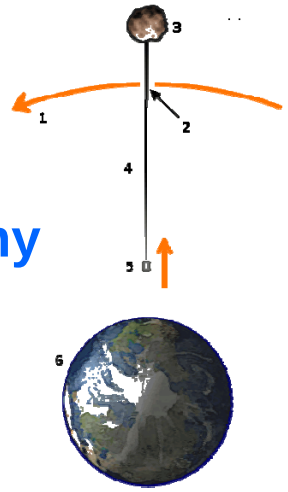

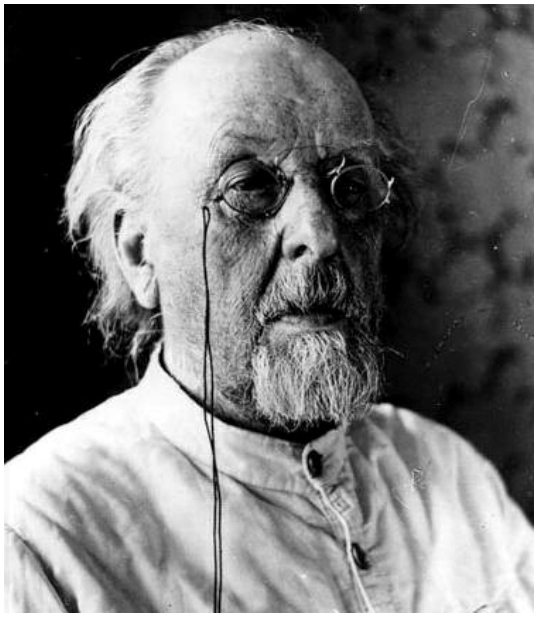

The key concept of the space elevator appeared in 1895 when russian scientist *Konstantin Tsiolkovsky* was inspired by the Eiffel Tower in Paris to consider a tower that reached all the way into space, built from the ground up to an altitude of 35790 km above sea level.

After discovery of *carbon nanotubes* in the 1991, engineers realized that the high strength of these materials might make the concept of an orbital skyhook feasible, and plan for an elevator to turning the concept into a reality

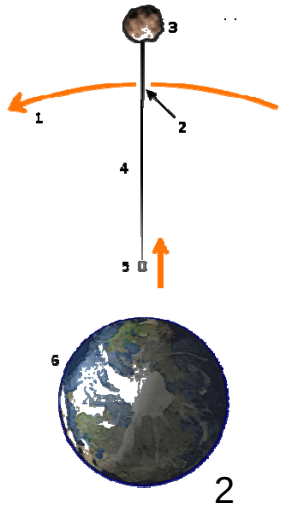

(see Science @ NASA, Audacious&Qutrageous:Space Elevators, Sept. 2000)

Carbon nanotubes were discovered in 1991 by the *japanese physicist*. *Iijima Sumio,* (born May 2, 1939).

Besides their small size, the carbon nanotubes are half as dense as aluminum, have tensile strengths 100 times that of steel alloys, have current carrying capacities 1000 times that of copper, and transmit heat twice as well as pure diamond.

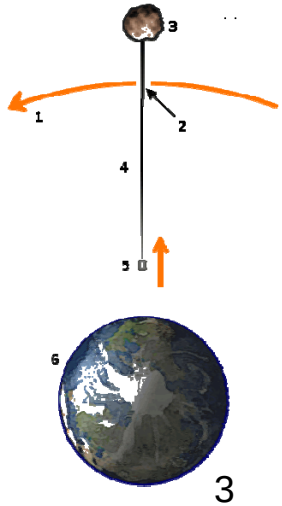

Iijima S 1991, *Helical microtubules of graphitic carbon*, Nature (London) **354**, 56–58.
Iijima S 1993, *Single-shell carbon nanotubes of 1-nm diameter*, Nature (London) **363**, 603–605.

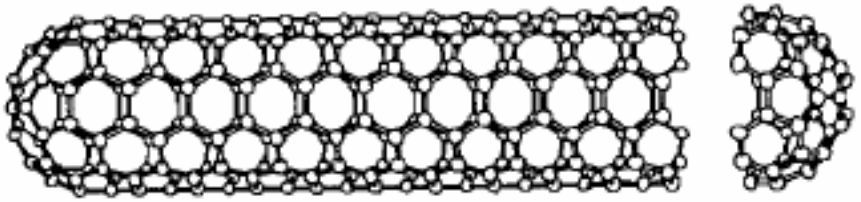

(5,5) armchair nanotube

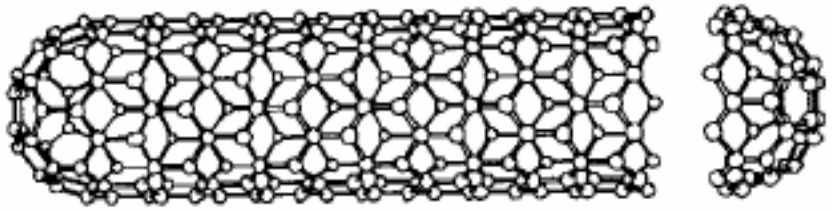

(9,0) zigzag nanotube

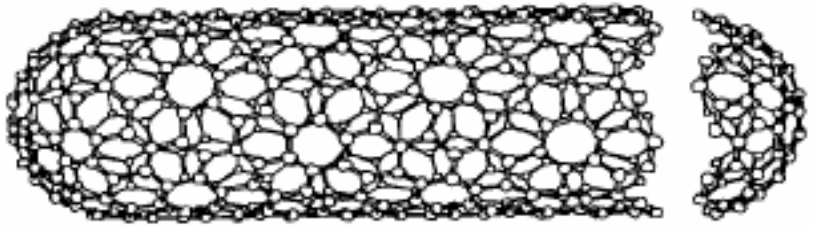

(10,5) chiral nanotube

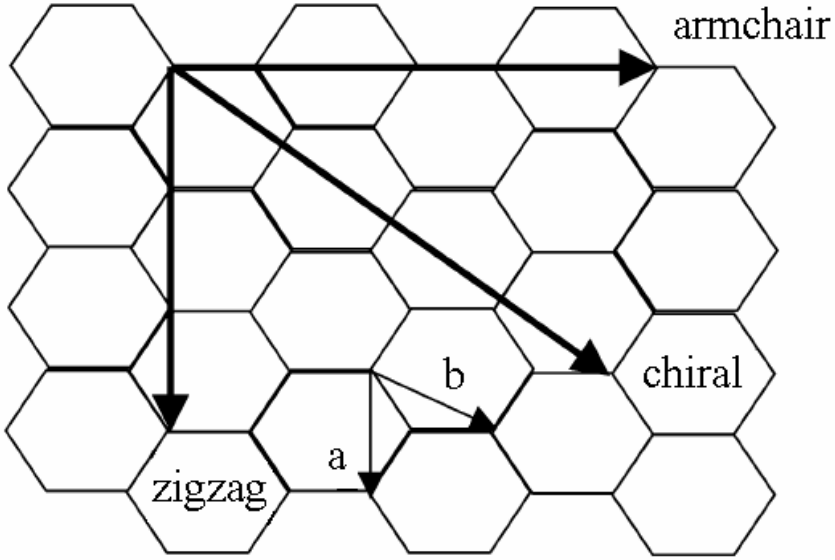

Definition of roll-up vector *r* as linear combination of base vectors *a* and *b*

r = na+mb

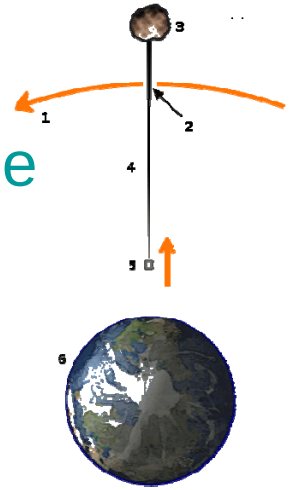

Material	Young's modulus [TPa]	Tensile Strength [GPa]	Bending modulus [TPa]
Single wall carbon nanotube (SWNT)	~ 1 - 5[E] depending of diameter	13 - 53[E]	0.2 - 2[E] depending of diameter
Armchair SWNT	0.94[T]	126.2[T]	0.4 – 1.4[E] depending of diameter
Zigzag SWNT	0.94[T]	94.5[T]	0.3 – 1.4[E] depending of diameter
Chiral SWNT	0.92[T]	95[T]	0.2 – 1.4[E] depending of diameter
Multiple walls carbon nanotube	0.8 - 0.9[E]	150	0.5 - 2[E] depending of diameter
Stainless Steel	~ 0.2	~ 0.65 - 1	~ 0.04
Kevlar	~0.15	~3.5	~ 0.01
Kevlar[T] [E]Experimental observation [T]Theoretical prediction	0.25	29.6	~ 0.01

(see D.Srivastava, C. Wei: *Nanomechanics of carbon nanotubes and composites*, Appl Mech Rev vol 56, no 2, March 2003)

In this paper we consider only the single-walled carbon nanotubes.

While multi-walled nanotubes are easier to produce and have similar tensile strengths, there is a concern that the interior tubes would not be sufficiently coupled to the outer tubes to help hold the tension.

If the nanotubes are long enough, *even weak Van der Waals forces* will be sufficient to keep them from slipping, and the full strength of individual nanotubes could be realized macroscopically by spinning them into a yarn.

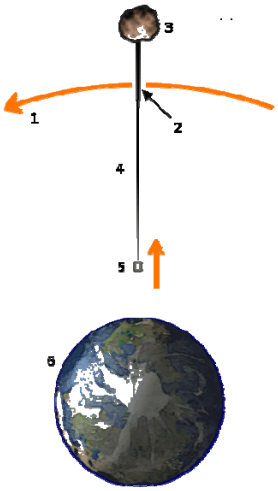

Carbon nanotubes have lengths of *tens to hundreds* of *microns*, far short of any macroscopic requirement.
The key is to get the carbon nanotubes into a composite : *ropes of carbon nanotube composites*

In polymeric composites, carbon nanotubes can reduce weight by a factor of 5-10, while increasing the strength by a factor of 5-10 compared to a conventional carbon fiber matrix , with ultra-strong individual fibers roughly 10 microns in diameter and lengths of many meters to kilometers, with uniform alignment of the nanotubes in the matrix, efficient stress transfer from the matrix to the nanotube, and attaining high nanotube loadings.

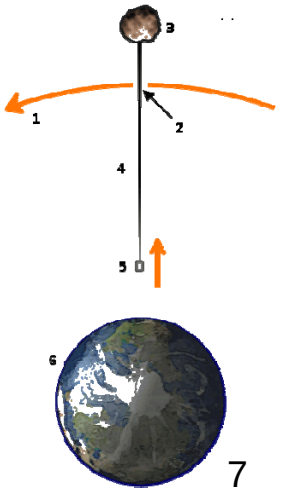

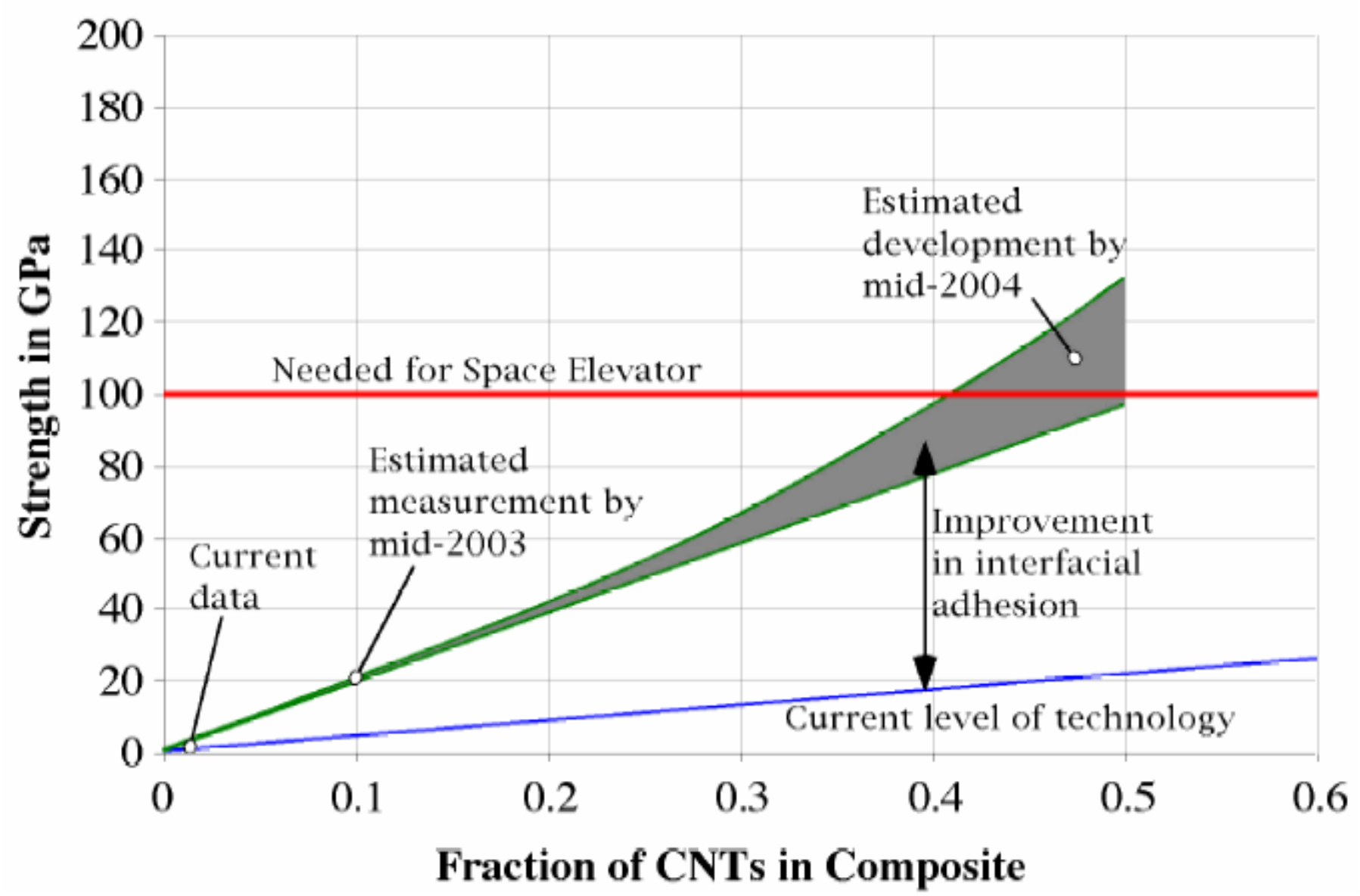

B.C.Edwards, *The space elevator NIAC Phase II*, Final report, 2005.

In this paper, the rope is composed from 6 subropes, each subrope being composed from 7 groups of single wall carbon nanotubes. Each group has 25 carbon nanotubes with two different radii (zigzag and armchair 6.26A, h = 0.617A and 16.33A, h = 0.998A), and the core group consists of 49 chiral carbon nanotube with the same radius (3.22A and h = 0.6A), into a polymeric matrix.

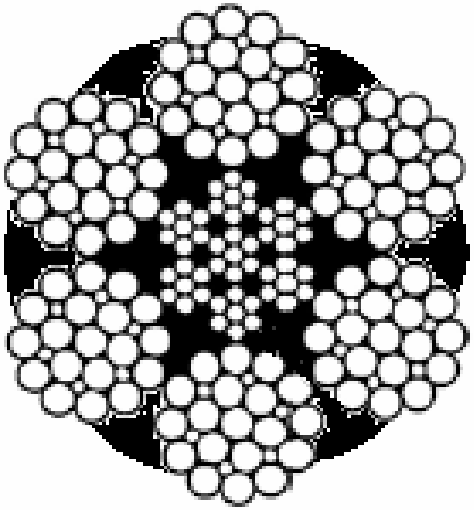

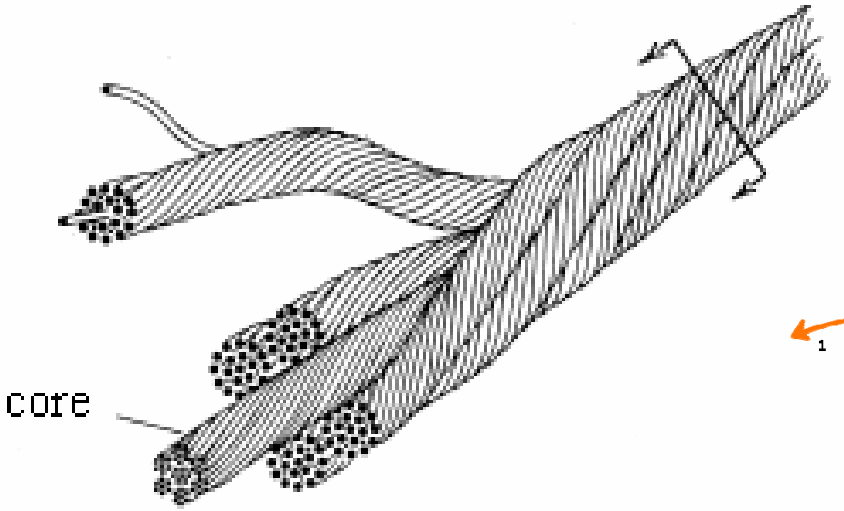

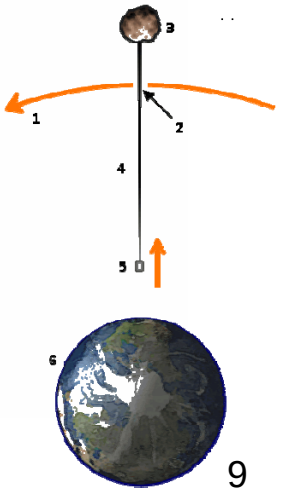

The bending of this carbon nanotube rope is described by a *coupled continuum –atomistic method*.

The continuum method is setup in the light of Cosserat elasticity, which admits degrees of freedom not present in classical elasticity: the rotation of points in the material, and a couple per unit area (couple stresses).

The atomistic method is used in the regions where the continuum method is no longer valid.

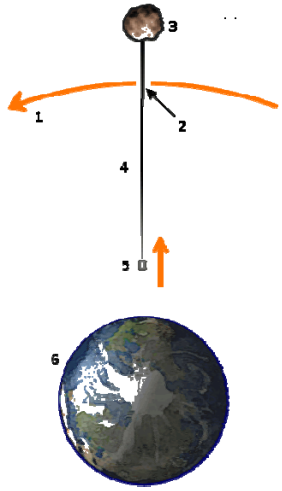

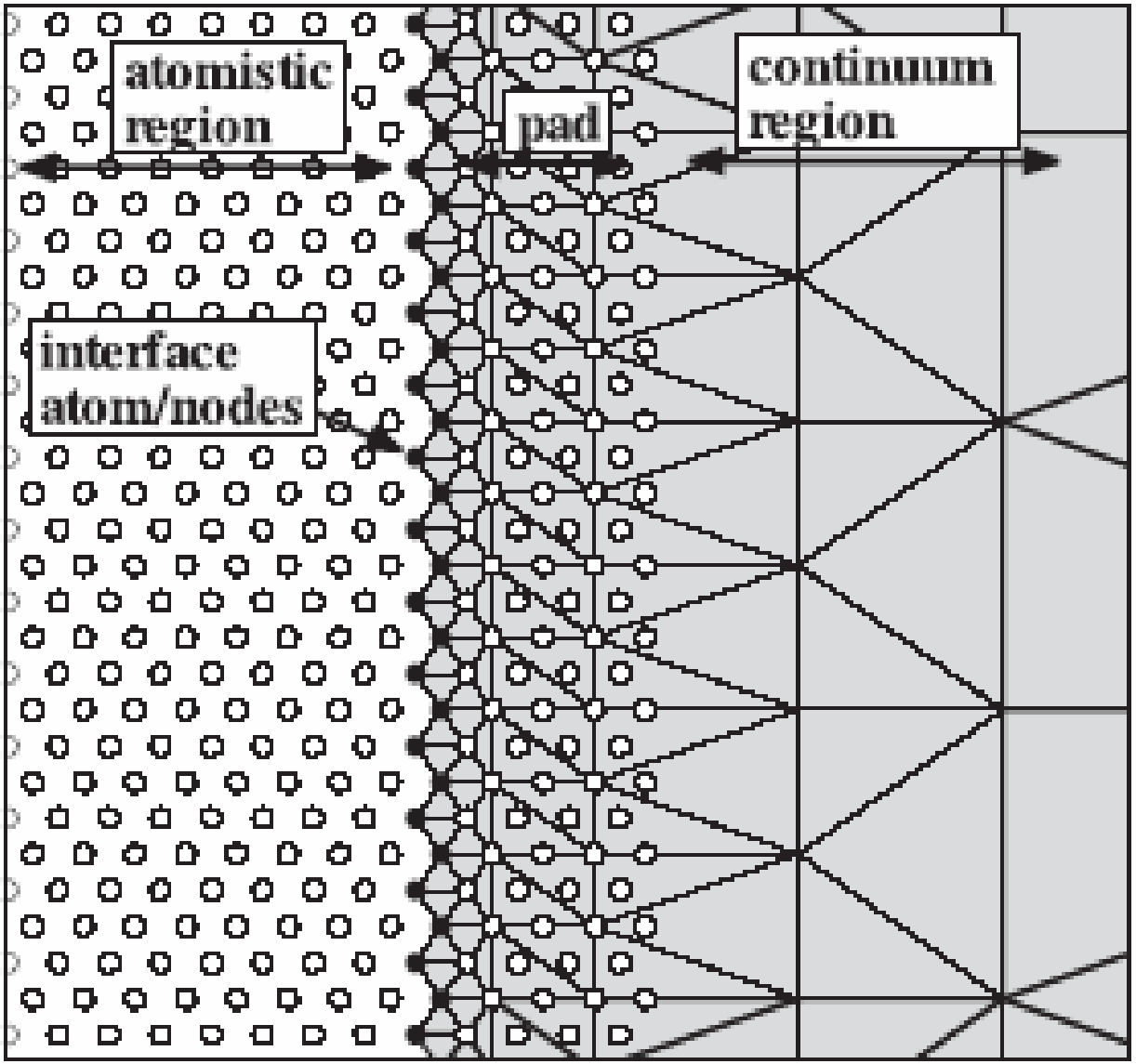

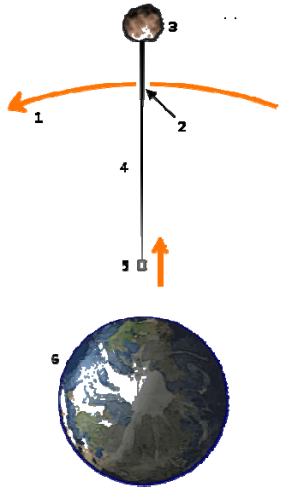

The generic form of the coupling atomistic-continuum regions.

The classical mechanics fail in describing the mechanical behavior of ***the carbon nanotube ropes*** under deformation. The rope is modeled as an *elastic chiral material* (noncentrosymmetric material) which *is isotropic with respect to coordinate rotations but not with respect to inversions*.

So these materials have a qualitatively different behavior in comparison with isotropic solids.

Chiral effects cannot be expressed within classical elasticity since the *modulus tensor*, which is fourth rank, is unchanged under an inversion

$$C_{ijkl} = \frac{\mathrm{d}x_m}{\mathrm{d}x_i}\frac{\mathrm{d}x_n}{\mathrm{d}x_j}\frac{\mathrm{d}x_o}{\mathrm{d}x_k}\frac{\mathrm{d}x_p}{\mathrm{d}x_l}C_{mnop} =$$

$$= (-1)\delta_{im}(-1)\delta_{jn}(-1)\delta_{ok}(-1)\delta_{pl}C_{mnop} = (-1)^4 C_{ijkl} = C_{ijkl}$$

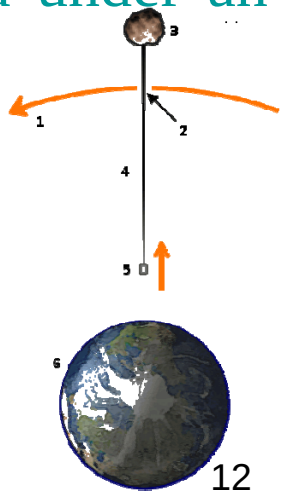

Constitutive equations for an isotropic centrosymmetric Cosserat solid

$$\sigma_{kl} = \lambda e_{rr}\delta_{kl} + (2\mu + \kappa)e_{kl} + \kappa\varepsilon_{klm}(r_m - \varphi_m) \qquad (1)$$

$$m_{kl} = \alpha\varphi_{r,r}\delta_{kl} + \beta\varphi_{k,l} + \gamma\varphi_{l,k} \qquad (2)$$

σ_{kl} is the stress tensor , m_{kl} is the couple stress tensor (moment per unit area),

$e_{kl} = \frac{1}{2}(u_{k.l} + u_{l,k})$ is the small strain tensor (macrostrain vector),

u is the displacement vector, ε_{klm} the permutation symbol.

φ_k the microrotation vector

r_k the macrorotation vector $r_k = \frac{1}{2}\varepsilon_{klm}u_{m,l}$

λ μ Lame elastic constants

κ Cosserat rotation modulus

α, β, γ Cosserat rotation gradient moduli

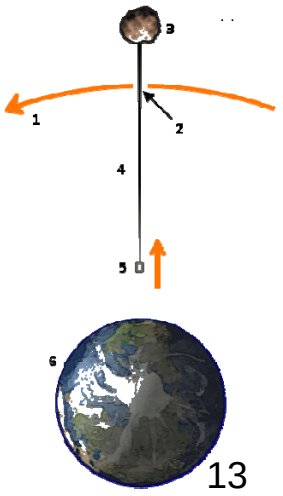

The constitutive equations for a anisotropic noncentrosymmetric Cosserat solid can be written in the form

$$\sigma_{kl} = \lambda e_{rr}\delta_{kl} + (2\mu + \kappa)e_{kl} + \kappa\varepsilon_{klm}(r_m - \varphi_m) + C_1\varphi_{r,r}\delta_{kl} + C_2\varphi_{k,l} + C_3\varphi_{l,k},$$

$$m_{kl} = \alpha\varphi_{r,r}\delta_{kl} + \beta\varphi_{k,l} + \gamma\varphi_{l,k} + C_1 e_{rr}\delta_{kl} + (C_2 + C_3)e_{kl} + (C_3 - C_2)\varepsilon_{klm}(r_m - \varphi_m),$$

C_1, C_2, C_3 positive or negative chiral elastic constants

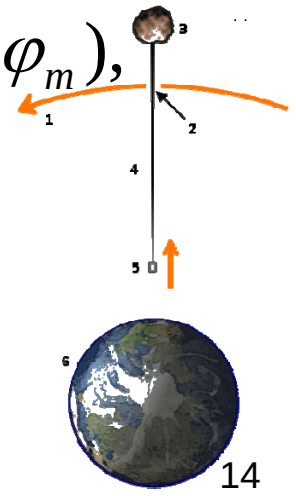

We take s to be the coordinate along the central line of the natural state. The orthonormal basis of the Lagrange coordinate system is denoted by (e_1, e_2, e_3) and the orthonormal basis of the Euler coordinate system by (d_1, d_2, d_3). The basis d is related to e by the Euler angles and θ, ψ and φ. These angles determine the orientation of the Euler axes relative to the Lagrange axes

$$d_1 = (-\sin\psi\sin\varphi + \cos\psi\cos\varphi\cos\theta)e_1 +$$
$$+ (\cos\psi\sin\varphi + \sin\psi\cos\varphi\cos\theta)e_2 - \sin\theta\cos\varphi e_3,$$

$$d_2 = (-\sin\psi\cos\varphi - \cos\psi\sin\varphi\cos\theta)e_1 +$$
$$+ (\cos\psi\cos\varphi - \sin\psi\sin\varphi\cos\theta)e_2 + \sin\theta\sin\varphi e_3,$$

$$d_3 = \sin\theta\cos\psi e_1 + \sin\theta\sin\psi e_2 + \cos\theta e_3.$$

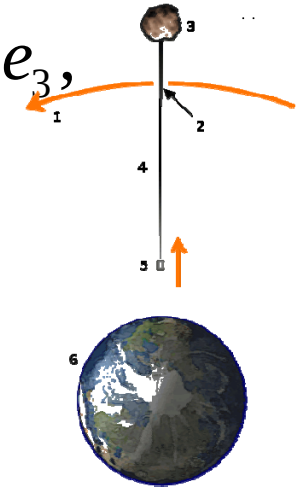

The *Z*-axis coincides with the central axis.

The motion of the rope is described by three vector functions

$$R \times R \ni (s,t) \to$$

$$\to r(s,t), d_1(s,t), d_2(s,t) \in E^3.$$

The material sections of the rod are identified by the coordinate ***s***. The position vector $r(s,t)$ can be interpreted as the image of the central axis in the Euler configuration.

The functions $d_1(s,t)$, $d_2(s,t)$ can be interpreted as defining the orientation of the material section ***s*** in the Euler configuration. The function

$$d_3(s,t) = d_1(s,t) \times d_2(s,t)$$

represents the unit tangential vector along the rope.

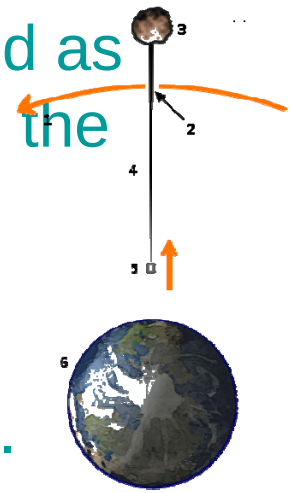

$$u_1 = \theta' \sin\varphi - \psi' \sin\theta \cos\varphi$$

$$u_2 = \theta' \cos\varphi + \psi' \sin\theta \sin\varphi$$

$$u_3 = \varphi' + \psi' \cos\theta$$

These functions measure the bending and torsion of the rope. *The first two* represent the components of the curvature of the central line ***k*** corresponding to the planes *yz* and *xz.*

$$\kappa^2 = u_1^2 + u_2^2 = \theta'^2 + \psi'^2 \sin^2\theta$$

The last is the torsion

$$u_3 = \tau = \varphi' + \psi' \cos\theta$$

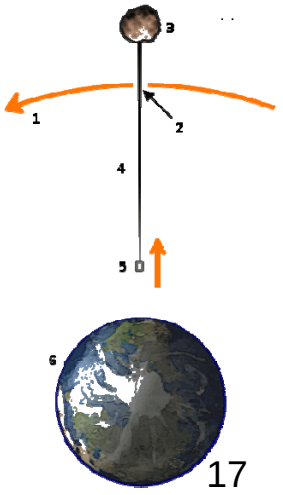

$$u = \cos\theta \qquad u'^2 = \frac{1-u^2}{K_0^2}\left\{-\frac{q^2\tau^2u^2 - p^2}{p^2(1-u^2)} + 2\lambda_3 u - \gamma\right\}$$

Weierstrass equation with a polynomial of third order

$$\frac{1}{2}u'^2 = f(u),$$

$$p^2 = \frac{2\kappa}{(\alpha+\beta+\gamma)}\frac{1}{(K_0^2-1)} \qquad q^2 = \frac{\kappa}{3(\alpha+\beta+\gamma)}\frac{1}{(K_0^2-1)^2}$$

$$K_0^2 = \frac{(C_1+C_2+C_3)^2}{(\alpha+\beta+\gamma)(\lambda+2\mu+\kappa)}$$

$$u = u_2 - (u_2-u_3)\mathrm{cn}^2[\alpha w(\xi-\xi_3), m], \qquad (1)$$

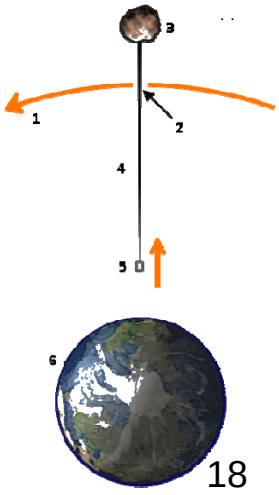

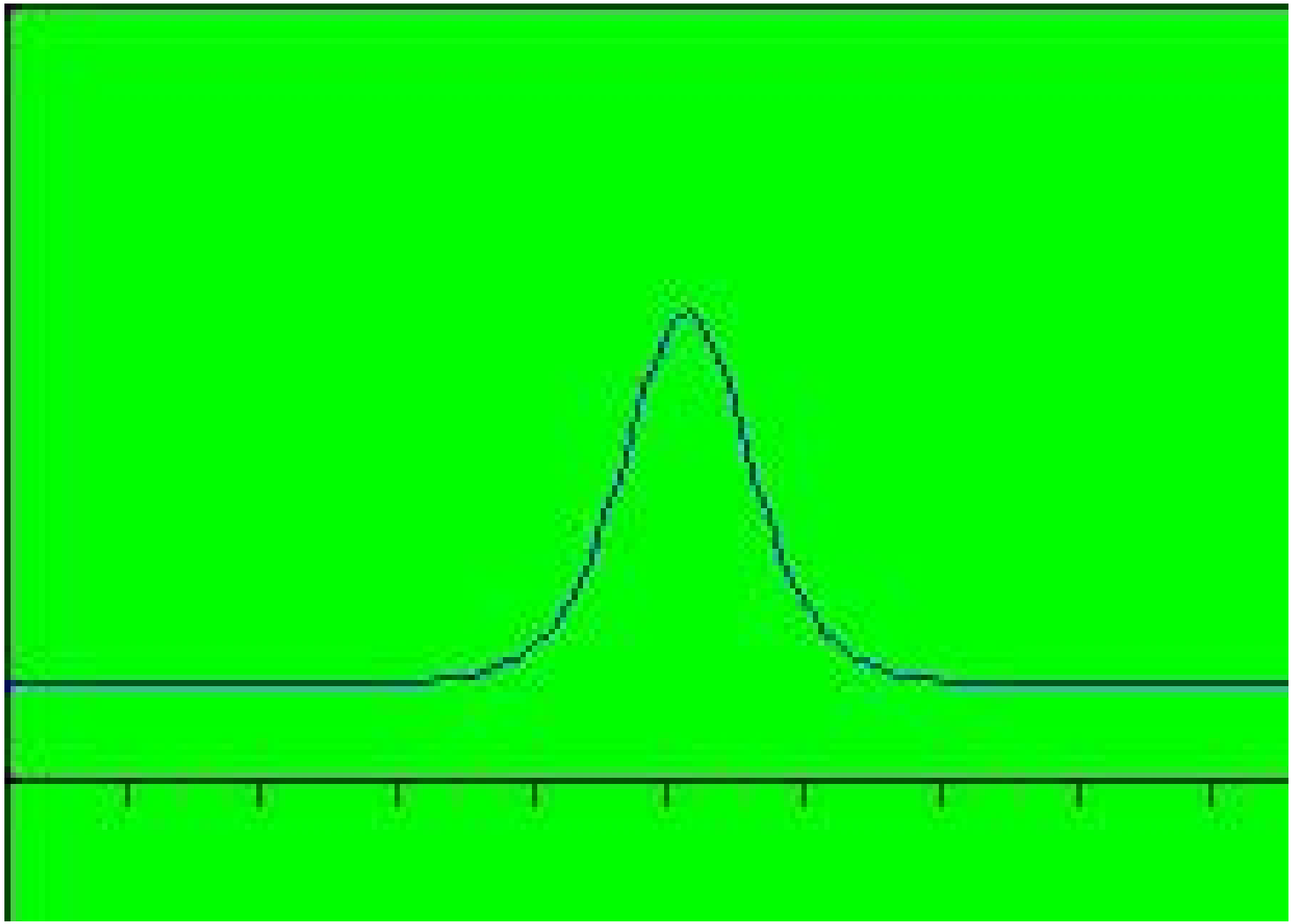

Solution single-soliton. The $u = \cos\theta$ wave propagates at a constant velocity without change of shape. The velocity depends on amplitude.

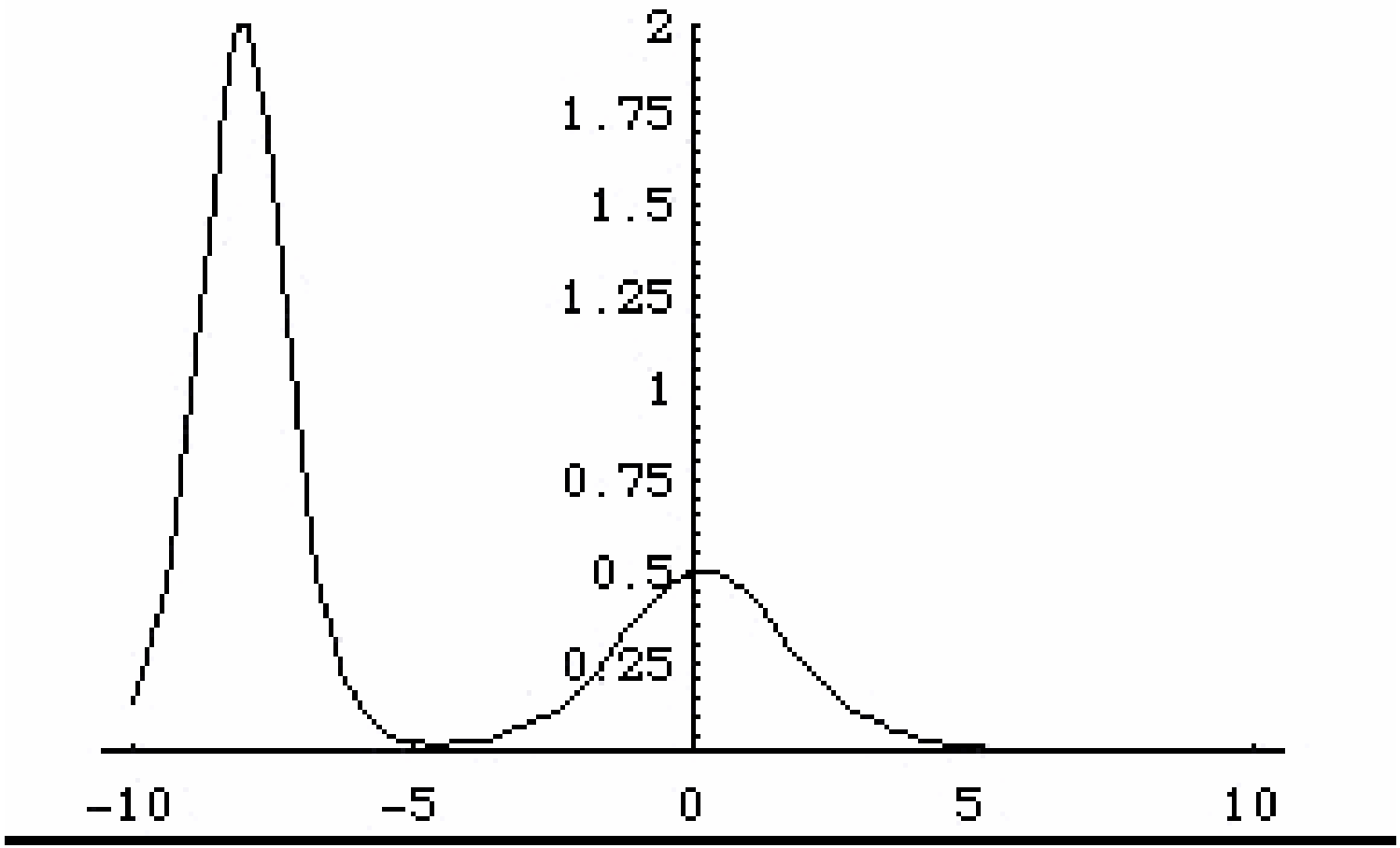

The general solution for $u = \cos\theta$ can be written as a nonlinear superposition of single solitons. Here is the superposition of 2 single solitons propagating in same direction (solution 2-solitons). A larger soliton travels with a high velocity so that it overtakes the smaller one and after collision they reappear without changing their form identity.

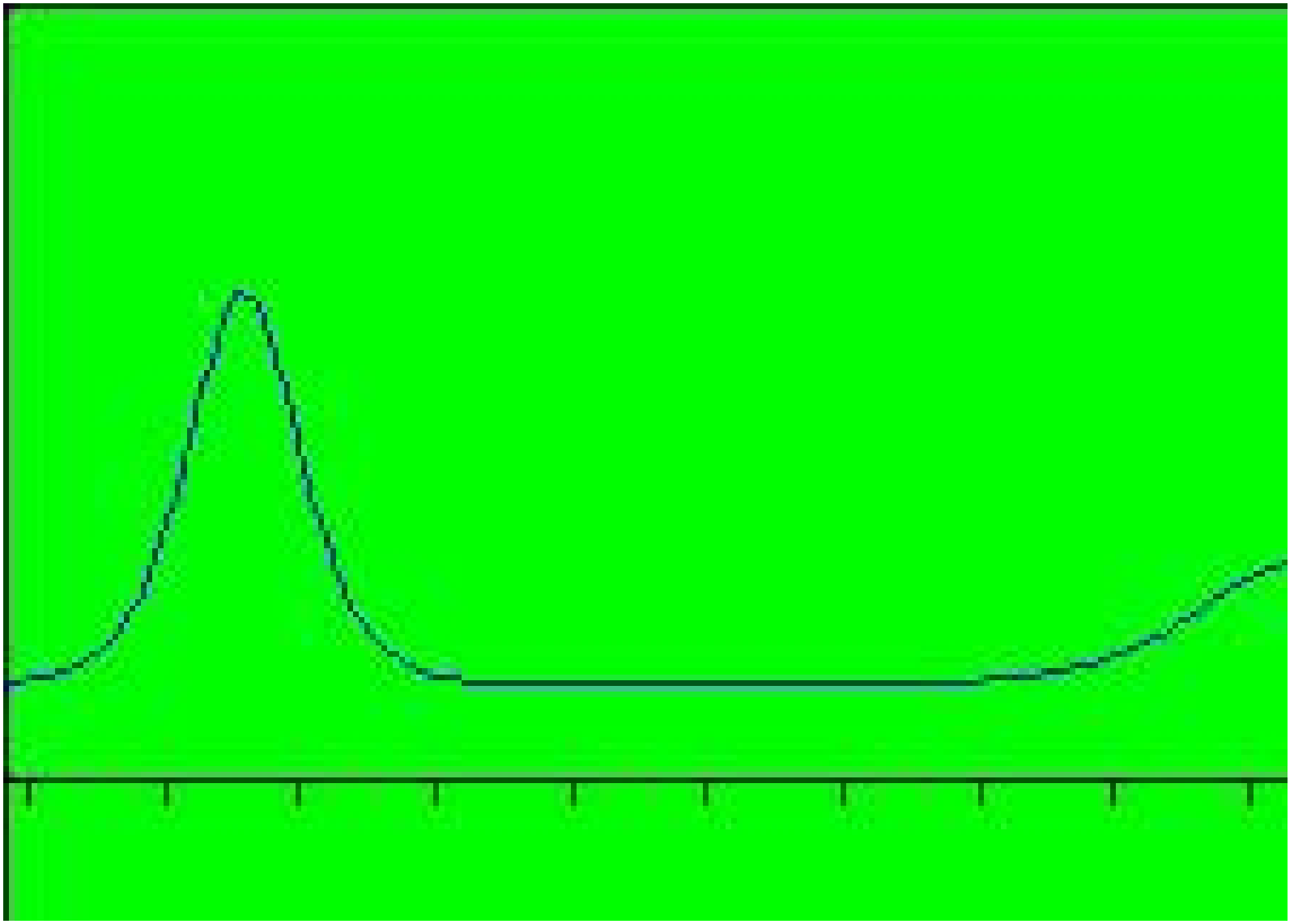

The superposition of two single solitons propagating in opposite directions..

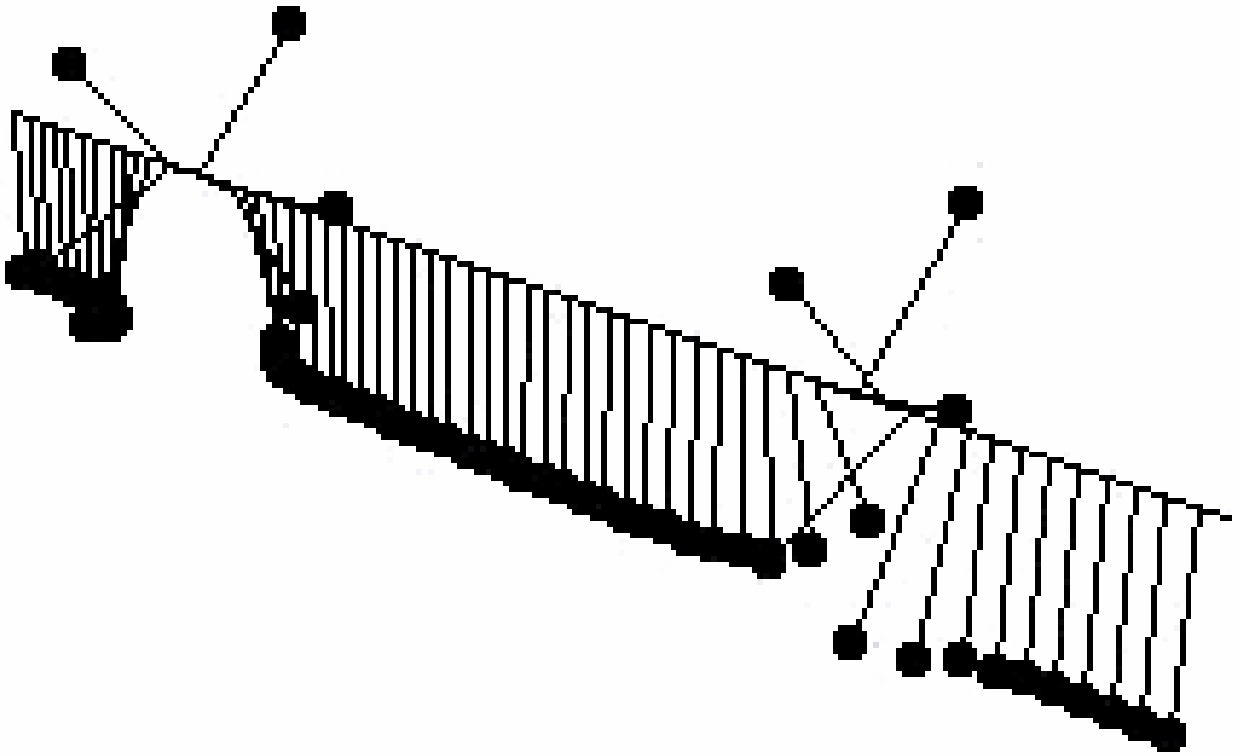

Animation of Alex Kasman (2001) by gratitude of the author (by Monica Soare) the Rensselaer Polytechnic Institute, Computational Nanomechanics Lab., Troy, New York (2004) – representing the nonlinear superpositions of solitons.

At the atomistic level, the total atomic energy E^a is obtained from classical potentials

$$E^a = \sum_i E_i$$

where E_i is the energy of the ***i***th atom $E_i = \frac{1}{2}\sum_{j \neq i} V(r_{ij})$

$V(r_{ij})$ is potential between ***i***-th and ***j***-th atoms of the neighbors, and r_{ij} is the interatomic distance. Forces on each atom, in the absence of external forces, are

$$f_i = -E^a_{,r_i}$$

where the comma means differentiation with respect to the atomic coordinates

$r_1, r_2, \ldots, r_N$

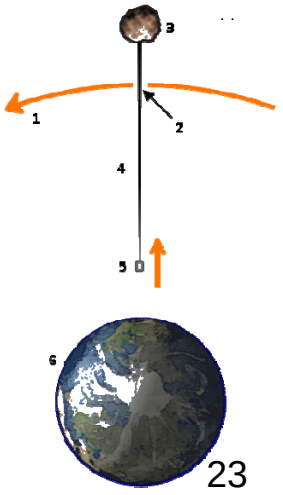

The van der Waals force between atom *i* and *j* can be expressed by the **Lennard-Jones potential as**

$$V(r_{ij}) = 4\varepsilon\left(\frac{\sigma^{12}}{r_{ij}^{12}} - \frac{\sigma^{6}}{r_{ij}^{6}}\right)$$

$\varepsilon = 4.7483 \cdot 10^{-19}\text{Nm}$ **depth of the potential well**

$\sigma = 3.407$ **finite distance at which the interparticle potential is zero**

The term $\left(\frac{1}{r}\right)^{12}$ **describes repulsion and the term** $\left(\frac{1}{r}\right)^{6}$ **describes attraction.**

The force function is the negative of the gradient of the above potential:

$$F(r) = -\nabla V(r) = -\frac{\mathrm{d}}{\mathrm{d}r}V(r)\hat{r}$$

The atomic simulations for carbon nanotubes armchair, zigzag and chiral, were performed by the courtesy of Monica Soare at the Rensselaer Polytechnic Institute, Computational Nanomechanics Lab., Troy, New York (2004) and Calin Chiroiu at the Politecnico di Torino, Structural Engineering dept. (2005) .

The comparisons of nonlinear chiral theory, the atomistic simulations and experimental results

➢Bethune DS, Kiang CH, Devries MS, Gorman G, Savoy R, Vazquez J, and Beyers R (1993), *Cobalt-catalyzed growth of carbon nanotubes with single-atomic-layerwalls*, *Nature (London)* **363**, 605–607. Saito R, Dresselhaus G, Dresselhaus MS (1998), *Physical Properties of Carbon Nanotubes*, Imperial College Press, London, 361, 201-234.

yields:

✓Neither the nonlinear theory, either the atomistic approach do not succeed to describe very well the realistic behavior of carbon nanotubes deformation at ***bending and torsion***. ***The nonlinear theory*** gives closer results in comparison with the experimental results only for ***torsion***. ***The atomistic theory*** gives closer results in comparison with the experimental results only for ***bending***.

In the case of bending, when the external bending moment increases, the axial compression in the tube increases too, and when the stress reaches a critical value, the tube will locally buckle. The nonlinear theory is valid up to the point of local buckling at $\vartheta = 25.58^{\circ}$

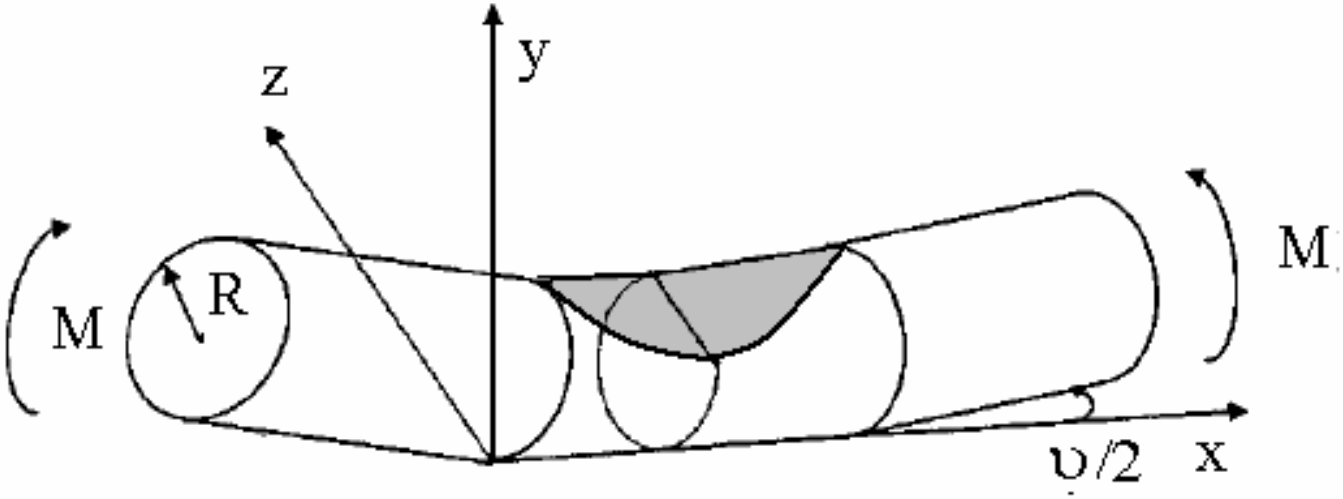

The definition of the bending angle.

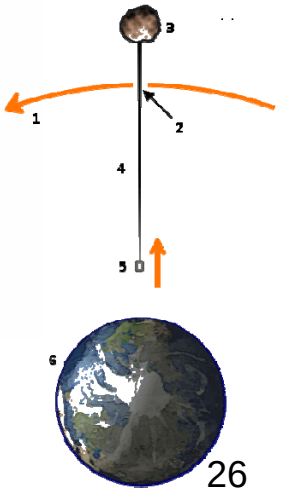

The gray region is discretized into 1024 nodal positions.

The pad region is used to relate the atomic numerical solutions to solitonic continuum solutions rewritten as a weighted superposition of exact solutions.

We use the Sinclair's analytical treatment of the continuum region of a ***weighted superposition of elementary soliton solutions that allowed the boundary conditions to be modified during the energy minimization of the atomistic region.***
The parameters are determined by means of **a genetic algorithm, from an objective function.**

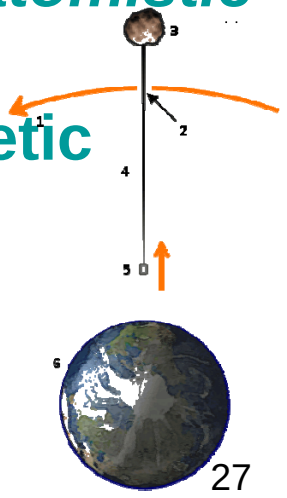

For $\vartheta > 25.58^{\circ}$, the coupled theory put into evidence a ***solitonic mechanism of deformation***. The pattern of the deformation resembles a mechanism similar to that of a macrotube, but in the nanotube case, this mechanism is ***described by means of solitons***.

A portion of the rope flattens and forms a domain that rotate about a central hinge line. The remaining part of the rope remains circular although it flattens and decreases its curvature.

Once the solitonic mechanism starts, the rope becomes a mechanical ***mechanism*** and the formulas in the continuum theory is no longer valid.

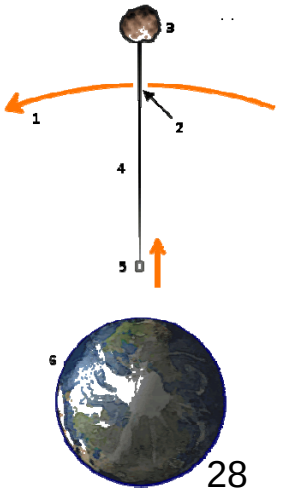

The *solitonic mechanism* of deformation it is characterized by :

1.The van der Waals force is the interaction between the opposite walls of the rope when they approach each other. This force depends on the distance between them. For large distances, the van der Waals force is attractive, but when the separation between the atoms is below the equilibrium distance of 3.42 Å, it becomes strongly repulsive.

2. With the increase in the bending angle, the the opposite walls get closer to each other, and at a certain stage, the distance between them reaches the equilibrium distance.

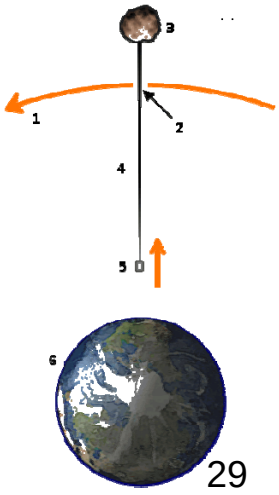

3. Upon additional bending, *this distance remains unchanged* because there are no extra loads applied on the walls to prevail over the repulsive van der Waals forces.
4. Upon complete unloading from angles below 109-110° the rope completely elastically recovers. At a very large bending angle of 118-120°, atomic bonds break and the deformation becomes irreversible.
5. The bending modulus is estimated to be 1.6TPa.

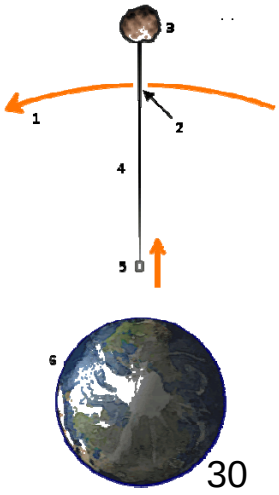

Bending nanotube zigzag (9,0) radius 6.26 A, thichness 0.617 A

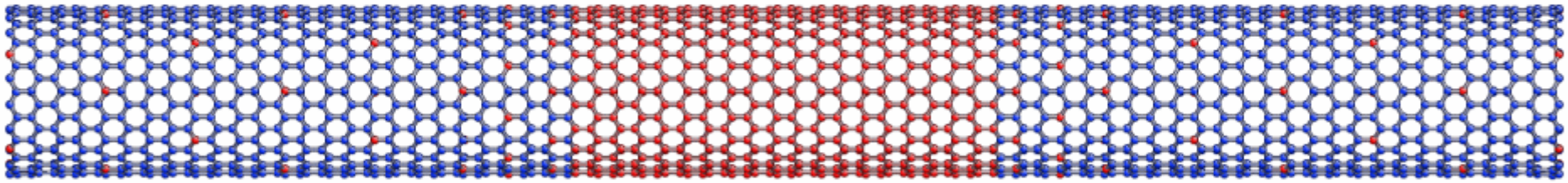

Single wall nanotube armchair (5,5) radius 6.26 A, thickness 0.677 A.

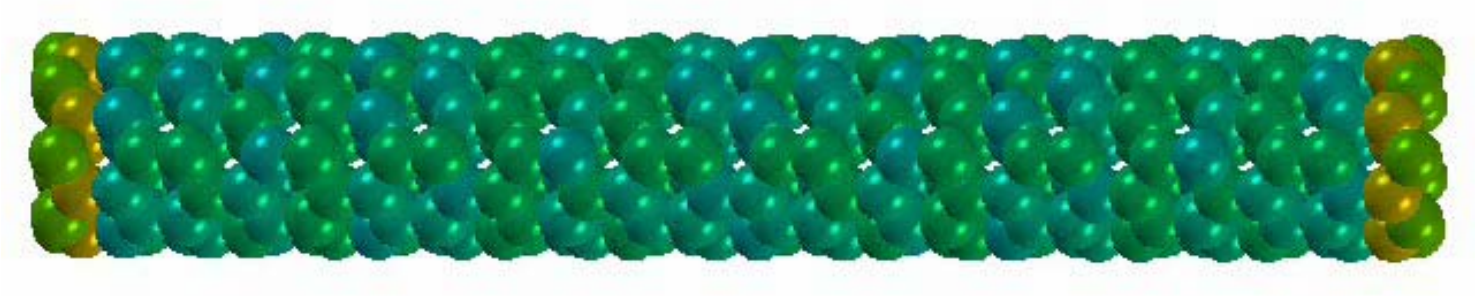

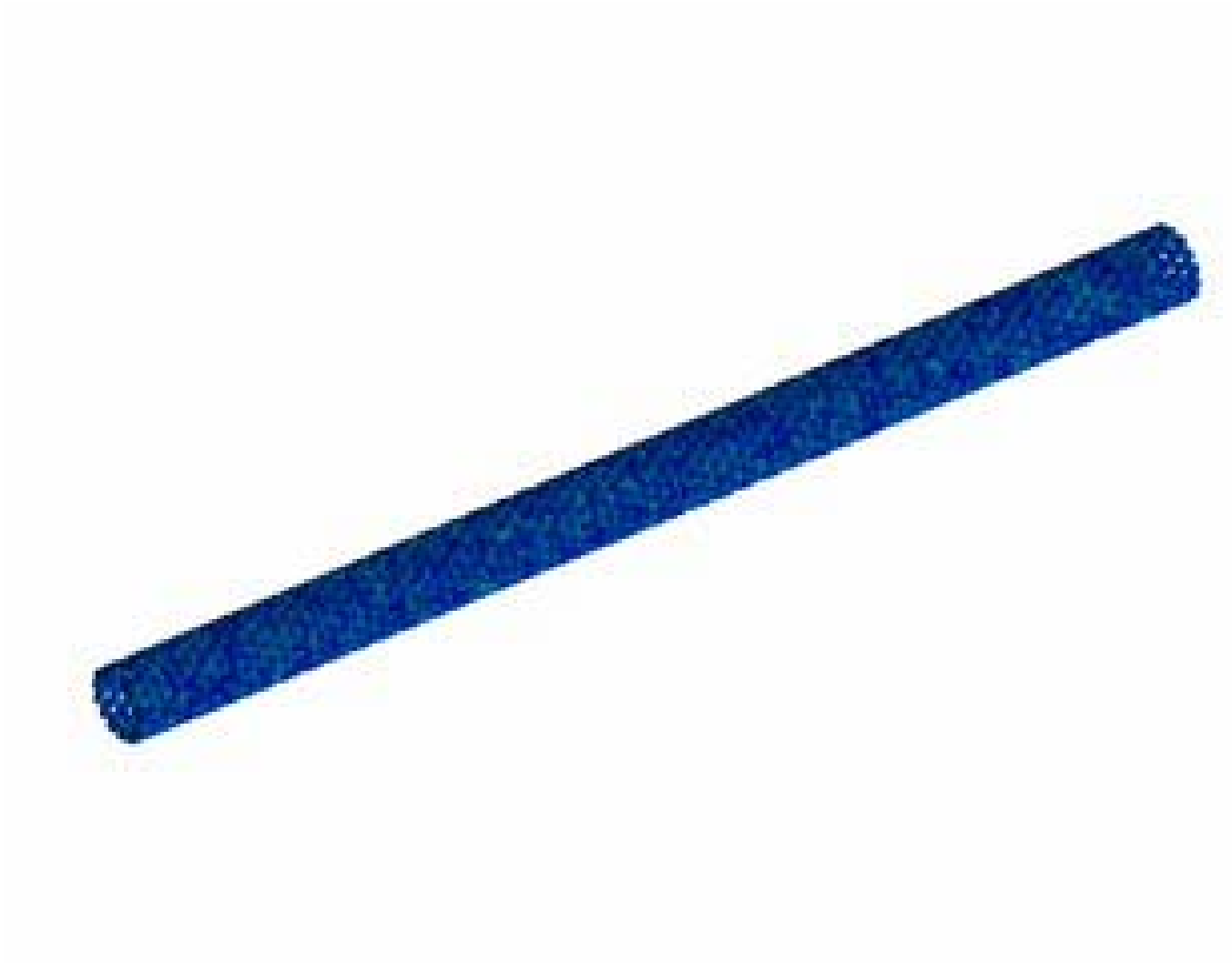

Single wall nanotube chiral (10,5) radius 3.22 A, thickness 0.6 A.

Nanotube zigzag (9,0) r =16.33A, thichness 0.998A

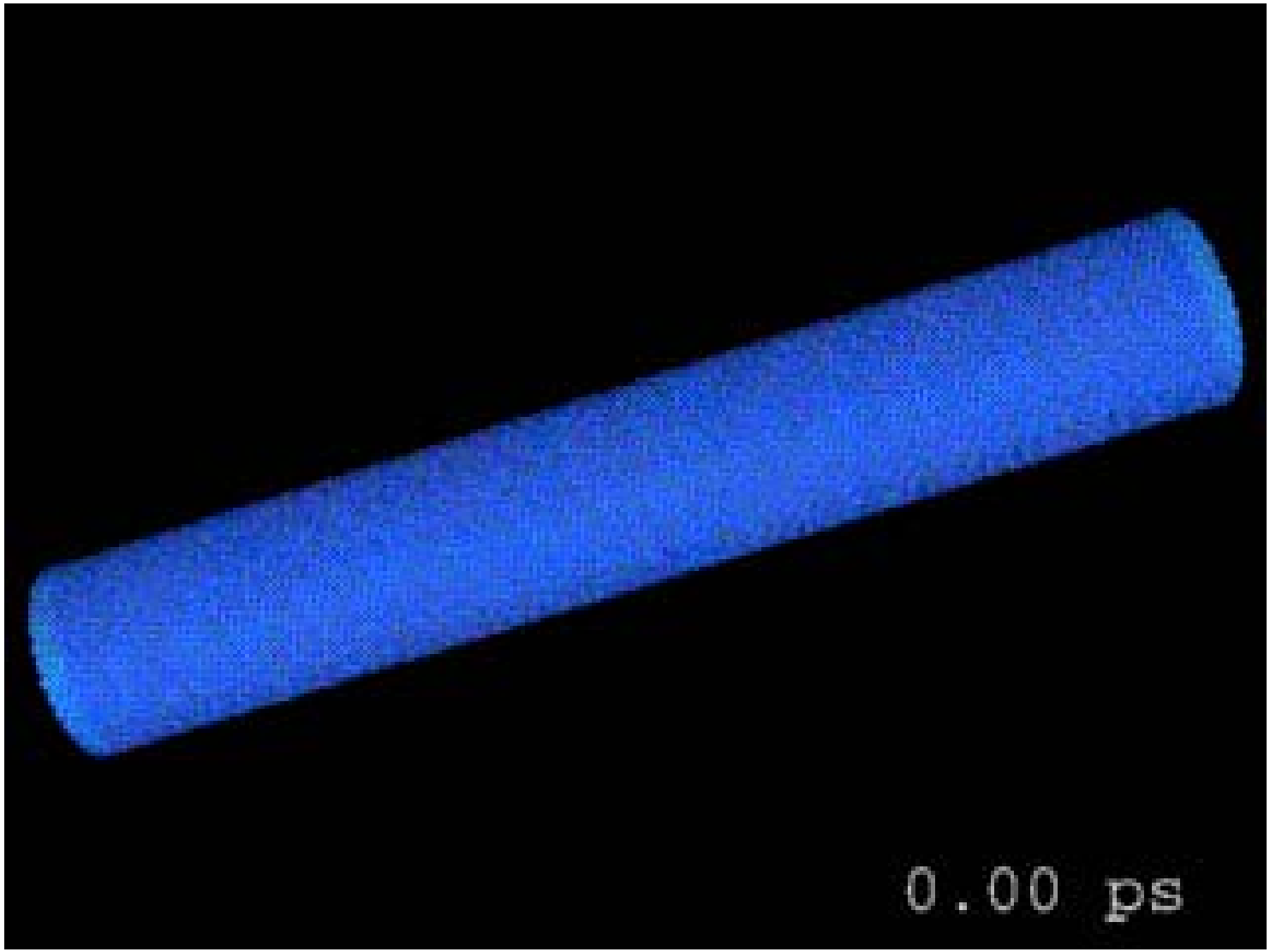

Nanotube armchair (5,5) radius 16.33A, h = 0.998A

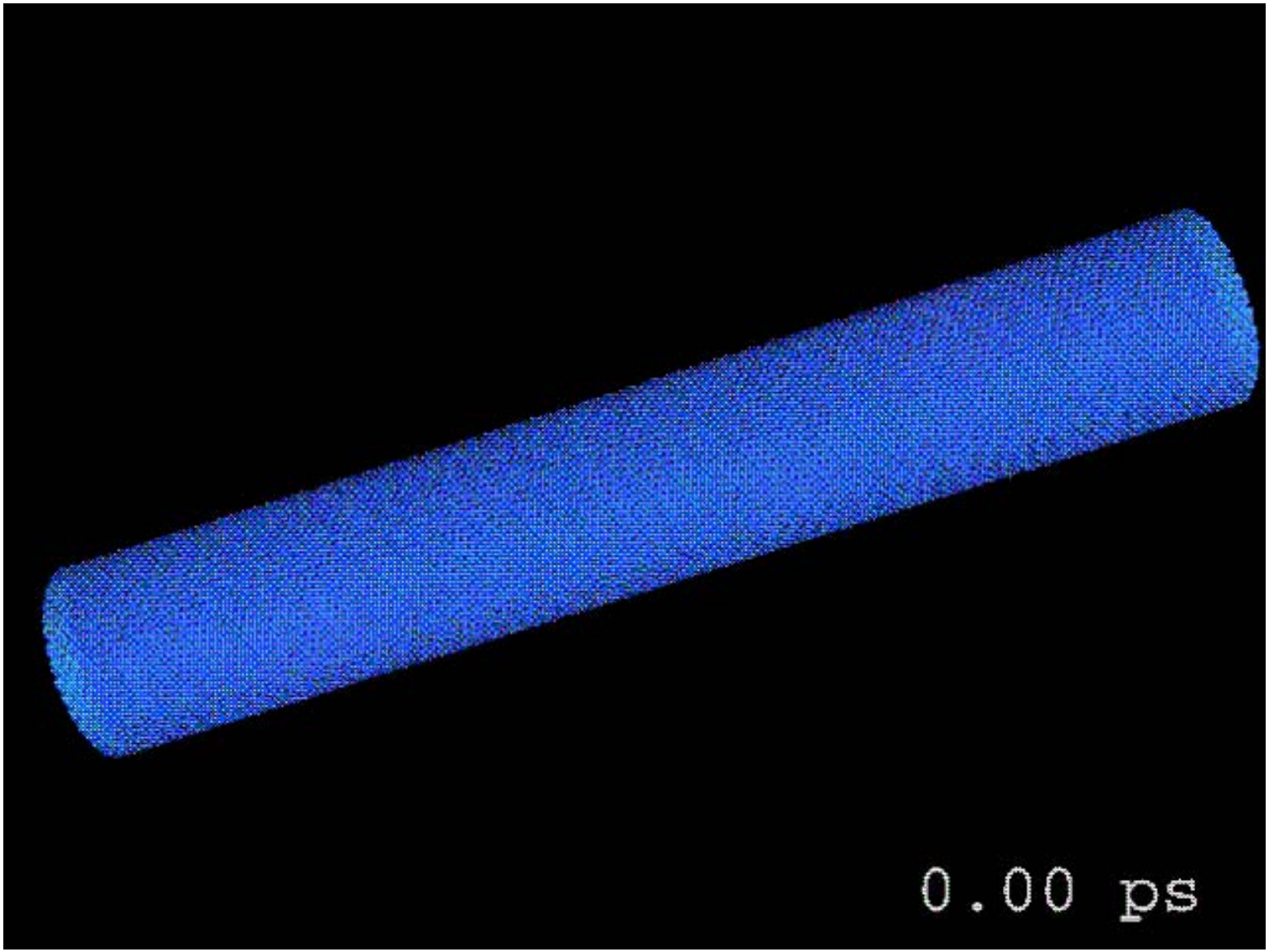

The end

Thank you for your attention

Acknowledgment.
This work reported in this paper is sponsored by the CEEX (MEdC-UEFISCSU) Post doctoral grant nr. 1531/2006, code 1, and this support is gratefully acknowledged.